0026-895X/11/7903-558–568$20.00
MOLECULAR PHARMACOLOGY
Copyright © 2011 The American Society for Pharmacology and Experimental Therapeutics
Mol Pharmacol 79:558–568, 2011

Vol. 79, No. 3
69658/3670267
Printed in U.S.A.

MOL PHARM

Nitric Oxide Stimulates NCX1 and NCX2 but Inhibits NCX3 Isoform by Three Distinct Molecular Determinants

Agnese Secondo, Pasquale Molinaro, Anna Pannaccione, Alba Esposito, Maria Cantile, Pellegrino Lippiello, Rossana Sirabella, Takahiro Iwamoto, Gianfranco Di Renzo, and Lucio Annunziato

Division of Pharmacology, Department of Neuroscience, School of Medicine, University of Naples "Federico II", Naples, Italy (A.S., P.M., A.P., A.E., M.C., P.L., G.D.R., L.A.), National Institute of Neuroscience, Italy (A.S., A.P., G.D.R., L.A.), Fondazione Istituto di Ricovero e Cura a Carattere Scientifico SDN, Naples, Italy (R.S., L.A.); and Department of Pharmacology, School of Medicine, Fukuoka University, Fukuoka, Japan (T.I.)

Received October 26, 2010; accepted December 13, 2010

ABSTRACT

In this study, the role of nitric oxide (NO) in the modulation of the activity of NCX1, NCX2, and NCX3 exchangers was investigated in baby hamster kidney cells singly transfected with each of these isoforms by single-cell Fura-2-microfluorometry and patch clamp. Furthermore, the molecular determinants of NO on each isoform were identified by deletion, site-directed mutagenesis, and chimera strategies. Our data revealed four main findings. First, the NO-donor *S*-nitroso-*N*-acetylpenicillamine (SNAP; 10 nM) and the NO-precursor L-arginine (10 mM) were both able to increase NCX1 activity in a cGMP-independent way. Moreover, within the amino acid sequence 723 to 734 of the f-loop, Cys730 resulted as the target of NO on NCX1. Second, SNAP and L-arginine were able to increase NCX2 activity, but this effect was prevented by the guanylate cyclase inhibitor 1*H*-[1,2,4]oxadiazolo[4,3-*a*]quinoxalin-1-one (ODQ). In addition, the membrane-permeable 8-bromoguanosine-cGMP alone was able to mimic the stimulatory effect of the gaseous mediator, suggesting the involvement of a cGMP-dependent mechanism. Within the amino acid sequence 699 to 744 of the f-loop, Ser713 was the NO molecular determinant on the NCX2 protein; Third, NCX3 activity was instead down-regulated by NO in a cGMP-independent manner. This NO-inhibitory action was exerted at the level of Cys156 in the α1-region outside the f-loop. Finally, the activity of the two NCX3 chimeras—obtained by the replacement of the NO-insensitive NCX3 region with the homologous NO-sensitive segments of NCX1 or NCX2—was potentiated by SNAP. Together, the present data demonstrate that NO differently regulates the activity of the three gene products NCX1, NCX2, and NCX3 by modulating specific molecular determinants.

Introduction

Ca^{2+} ions play a crucial role in controlling a large number of cellular processes, including migration, proliferation, apoptosis, neurotransmitter release, and neuronal synaptic plasticity (Berridge et al., 2000). Complex patterns regulate the specificity of Ca^{2+} signaling through the activity of plasma membrane channels and transporters, including the Na^+/Ca^{2+} exchanger (NCX). For instance, this bidirectional high-capacity and low-affinity ionic transporter, by exchanging three Na^+ ions for one Ca^{2+} ion (Sanchez-Armass and Blaustein, 1987; Annunziato et al., 2004), plays a relevant role in maintaining intracellular free Ca^{2+} homeostasis. Three different gene products of NCX have been cloned (Nicoll et al., 1990, 1996; Li et al., 1994): NCX1, which is the only isoform expressed in the heart and is ubiquitously expressed in several tissues, and NCX2 and NCX3, which are widely expressed in the brain (Papa et al., 2003) and in the skeletal muscle (Lee et al., 1994). Recent evidence has shown that the three NCX isoforms play a differential role in several neurodegenerative diseases, such as brain ischemia (Pignataro et al., 2004; Boscia et al., 2006; Secondo et al., 2007; Molinaro et al., 2008; Sirabella et al., 2009), Alzheimer's disease

This work was supported by Cofinanziamento 2008 [Grant COFIN 2008]; and by the Ministero Affari Esteri, Direzione Generale per la Promozione e la Cooperazione Culturale Fondi Italia-Cina, 2008 [Grant Legge 401/1990]; Ministero della Salute, Ricerca Sanitaria Ricerca finalizzata, 2006 [Grant RF-FSL352059]; Ministero della Salute, Ricerca Oncologica 2006; Ministero della Salute, Progetto Strategico, 2007; and Ministero della Salute, Progetto Ordinario, 2007.

A.S., P.M., and A.P. contributed equally to this work and should be considered co-first authors.

Article, publication date, and citation information can be found at http://molpharm.aspetjournals.org.

doi:10.1124/mol.110.069658.

ABBREVIATIONS: NCX, Na^+-Ca^{2+} exchanger; BHK, baby hamster kidney; ODQ, 1*H*-[1,2,4]oxadiazolo[4,3-*a*]quinoxalin-1-one; SNAP, *S*-nitroso-*N*-acetylpenicillamine; AM, acetoxymethyl ester; TEA, tetraethylammonium; nNOS, neuronal nitric-oxide synthase; eNOS, endothelial nitric-oxide synthase; DAF-2DA, 4,5-diaminofluorescein-2-diacetate; Wt, wild type; PKG, cGMP-dependent kinase; NMDG+, *N*-methyl-D-glucamine$^+$.

MOLECULAR PHARMACOLOGY
aspet
Downloaded from molpharm.aspetjournals.org by guest on December 1, 2012

MOL PHARM

MOLECULAR PHARMACOLOGY

(Wu et al., 1997; Peers et al., 2004), and multiple sclerosis (Inglese et al., 2010), by contributing to the maintenance of ionic homeostasis and cell survival (Secondo et al., 2007; Sirabella et al., 2009).

It is noteworthy that several intracellular and extracellular transduction mechanisms such as Na^+ and Ca^{2+}, intracellular pH values, Akt/protein kinase B, protein kinase A, protein kinase C, and reactive oxygen species, which are all involved in the pathophysiology of neurodegenerative diseases, also function as regulatory factors of the Na^+/Ca^{2+} exchanger activity (Annunziato et al., 2004; Formisano et al., 2008). Among these transductional mechanisms, nitric oxide (NO) has been suggested as a possible candidate for the regulation of NCX activity (Furukawa et al., 1991; Asano et al., 1995; Nagano et al., 2004). On the other hand, it has already been demonstrated that NO can regulate numerous classes of ion channels and ion-transporting mechanisms involved in the maintenance of intracellular Na^+ and Ca^{2+} homeostasis in the central nervous system. In particular, NO can interact with the sodium-potassium pump (Na^+/K^+ ATPase); with plasma membrane channels, including voltage-dependent calcium channels, voltage-dependent tetrodotoxin-sensitive Na^+, ether-a-go-go-related K^+ (Taglialatela et al., 1999; Secondo et al., 2006) and voltage-dependent at big- and small-conductance Ca^{2+}-dependent K^+ channels (Brakemeier et al., 2003); and, finally, with intracellular ligand-gated calcium channels, such as inositol trisphosphate- and ryanodine-sensitive channels (Annunziato et al., 2002). In all of these cases, NO acts by either activating or inhibiting these ionic-controlling mechanisms (Taglialatela et al., 2001; Annunziato et al., 2002; Francis et al., 2010).

Considering the relevant role played by the NCX isoforms and NO in the maintenance of ionic homeostasis and in the regulation of several cellular functions under physiological and pathophysiological conditions, the aims of the present study were 1) to characterize the effect of NO on the activity of each NCX isoform in BHK cells stably transfected with NCX1, NCX2, and NCX3 by means of Fura-2 microfluorometry and patch clamp, 2) to investigate the transductional mechanisms underlying NO-mediated effects on NCX isoforms, and 3) to identify, by means of deletion and site-directed mutagenesis and the generation of chimeric Na^+/Ca^{2+} exchangers, the molecular determinants of NO on each of the three isoforms.

Materials and Methods

Cell Culture. BHK cells stably transfected with canine cardiac NCX1, rat brain NCX2, or NCX3 were grown on plastic dishes in a mix of Dulbecco's modified Eagle's medium and Ham's F12 media (1:1; Invitrogen, San Giuliano Milanese, Italy) supplemented with 5% fetal bovine serum, 100 U/ml penicillin, and 100 μg/ml streptomycin (Sigma-Aldrich, St. Louis, MO). Cells were cultured in a humidified 5% CO_2 atmosphere; the culture medium was changed every 2 days. For microfluorometric and electrophysiological studies, cells were plated on glass coverslips (Thermo Fisher Scientific, Waltham, MA) coated with poly(L-lysine) (30 μg/ml; Sigma-Aldrich) and used at least 12 h after seeding.

Generation and Stable Expression of Wild-Type, Mutant, and Chimeric Na^+/Ca^{2+} Exchangers. Dog heart NCX1.1, rat brain NCX2.1, and NCX3.3 cDNAs, all generous gifts from Dr. Kenneth Philipson (University of California, Los Angeles, Los Angeles, CA), were cloned into pcDNA3.1 expression vector. NCX1, NCX2, and NCX3 mutants were generated by means of QuikChange site-directed mutagenesis kit (Stratagene, La Jolla, CA). The amino acid regions 246 to 680, 269 to 662, and 292 to 708 were deleted from NCX1, NCX2, and NCX3, respectively. All other mutants of NCX1, NCX2, and NCX3 were obtained as described above. Successful construction of the modified cDNAs was verified by sequencing (Primm, Milan, Italy). Wild-type, mutant, and chimeric exchangers were stably transfected in the BHK cell line by Lipofectamine 2000 (Invitrogen, Carlsbad, CA) protocol. Stable cell lines were selected by G418 resistance and by a Ca^{2+}-killing procedure (Iwamoto et al., 1998).

Nitric Oxide Detection with 4,5-Diaminofluorescein-2-diacetate Assay. Cells were loaded with 10 μM 4,5-diaminofluorescein-2-diacetate (DAF-2DA) in a humidified 5% CO_2 atmosphere at 37°C for 20 min in Normal Krebs' solution (5.5 mM KCl, 160 mM NaCl, 1.2 mM $MgCl_2$, 1.5 mM $CaCl_2$, 10 mM glucose, and 10 mM HEPES-NaOH, pH 7.4) containing the drugs or their vehicles, as described previously (Melisi et al., 2006). Thereafter, fluorescent cells were fixed with 4% (w/v) paraformaldehyde in phosphate-buffered saline for 5 min at 4°C. This procedure permits a subsequent densitometric analysis with the fluorescence microscope Nikon Eclipse E400 (Nikon, Torrance, CA) set at an excitation/emission wavelength of 495/515 nm. Fluorescent images were then stored and analyzed with Pro-Plus software (Media Cybernetics, Silver Spring, MD). Data were calculated as the percentage of sample fluorescence compared with that of controls.

$[Ca^{2+}]_i$ Measurement. $[Ca^{2+}]_i$ was measured by single-cell computer-assisted videoimaging. In brief, BHK cells were loaded with 10 μM Fura-2 acetoxymethyl ester (Fura-2/AM) for 30 min at 37°C in normal Krebs' solution containing the following: 5.5 mM KCl, 160 mM NaCl, 1.2 mM $MgCl_2$, 1.5 mM $CaCl_2$, 10 mM glucose, and 10 mM HEPES-NaOH, pH 7.4. At the end of the Fura-2/AM loading period, the coverslips were placed into a perfusion chamber (Medical System, Co. Greenvale, NY) mounted onto the stage of an inverted Zeiss Axiovert 200 microscope (Carl Zeiss GmbH, Jena, Germany) equipped with a FLUAR 40× oil objective lens. The experiments were carried out with a digital imaging system consisting of a MicroMax 512BFT cooled charge-coupled device camera (Princeton Instruments, Trenton, NJ), a LAMBDA 10-2 filter wheeler (Sutter Instrument Company, Novato, CA), and a Meta-Morph/MetaFluor Imaging System software (Molecular Devices, Sunnyvale, CA). After loading, cells were alternatively illuminated at wavelengths of 340 and 380 nm by a xenon lamp. The emitted light was passed through a 512-nm barrier filter. Fura-2 fluorescence intensity was measured every 3 s. Forty to sixty-five individual cells were selected and monitored simultaneously from each coverslip. All of the results were presented as cytosolic Ca^{2+} concentrations. Assuming that the K_D for FURA-2 was 224 nM, the equation of Grynkiewicz et al. (1985) was used for calibration. NCX activity was evaluated as Ca^{2+} uptake through the reverse mode by switching the normal Krebs' medium to Na^+-deficient $NMDG^+$ medium (Na^+-free): 5.5 mM KCl, 147 mM *N*-methyl glucamine, 1.2 mM $MgCl_2$, 1.5 mM $CaCl_2$, 10 mM glucose, and 10 mM HEPES, pH 7.4. These experiments were performed in the presence of the irreversible and selective inhibitor of the sarco-(endo)plasmic reticulum Ca^{2+} ATPase thapsigargin (1 μM), as described previously (Secondo et al., 2007).

Electrophysiology. I_{NCX} was recorded by the patch-clamp technique in whole-cell configuration, as reported previously (Molinaro et al., 2008). Currents were filtered at 5 kHz and digitized using a Digidata 1322A interface (Molecular Devices). Data were acquired and analyzed using the pClamp software (version 9.0; Molecular Devices). The I_{NCX} was recorded starting from a holding potential of −60 mV to a short-step depolarization at +60 mV (60 ms) (He et al., 2003). Then, a descending voltage ramp from +60 to −120 mV was applied. The current recorded in the descending portion of the ramp (from +60 to −120 mV) was used to plot the current-voltage (I-V) relation curve. The magnitudes of I_{NCX} were measured at the end of +60 mV (reverse mode) or +10 mV (only for NCX1) and at the end of −120 mV (forward mode), respectively. Because Ni^{2+} blocks I_{NCX}, $NiCl_2$ (5 mM) was routinely added to measure the NCX-independent

Downloaded from molpharm.aspetjournals.org by guest on December 1, 2012

currents. The Ni^{2+}-insensitive components were subtracted from total currents to isolate I_{NCX}. Cells were perfused with external Ringer solution containing 126 mM NaCl, 1.2 mM $NaHPO_4$, 2.4 mM KCl, 2.4 mM $CaCl_2$, 1.2 mM $MgCl_2$, 10 mM glucose, and 18 mM $NaHCO_3$, pH 7.4. Tetraethylammonium (TEA; 20 mM), 50 nM tetrodotoxin, and 10 μM nimodipine were added to the Ringer's solution to block TEA-sensitive K^+, tetrodotoxin-sensitive Na^+, and L-type Ca^{2+} currents. The dialyzing pipette solution contained 100 mM potassium gluconate, 10 mM TEA, 20 mM NaCl, 1 mM magnesium ATP, 0.1 mM $CaCl_2$, 2 mM $MgCl_2$, 0.75 mM EGTA, and 10 mM HEPES, adjusted to pH 7.2 with $Cs(OH)_2$. Possible changes in cell size occurring upon specific treatments were calculated by monitoring the capacitance of each cell membrane, which is directly related to membrane surface area, and by expressing the current amplitude data as current densities (measured in picoamperes per picofarad). Capacitive currents were estimated from the decay of capacitive transients induced by 5-mV depolarizing pulses from a holding potential of −80 mV and acquired at a sampling rate of 50 kHz. The membrane capacitance was calculated according to the following equation: $C_m = \tau_c \cdot I_o/\Delta E_m(1 - I_\infty/I_o)$, where C_m is membrane capacitance, τ_c is the time constant of the membrane capacitance, I_o is the maximum capacitive current value, ΔE_m is the amplitude of the voltage step, and I_∞ is the amplitude of the steady-state current.

Western Blot Analysis. Stably transfected BHK cells were lysed with a buffer containing 20 mM Tris-HCl, pH 7.5, 150 mM NaCl, 1% Nonidet P-40, 1 mM Na_3VO_4, 1 mM phenylmethylsulfonyl fluoride, 10 mM NaF, and a protease inhibitor cocktail (0.1% aprotinin, 1 μg/ml leupeptin, 0.7 mg/ml pepstatin) (Roche Diagnostics, Monza, Italy). After centrifugation at 13.400 rpm at 4°C for 20 min, the supernatants were collected. Protein concentration was estimated using the Bradford reagent (Bio-Rad Laboratories, Segrate, Milan, Italy). Then, 100 μg of protein was mixed with a Laemmli sample buffer. The samples were separated on 8% SDS-polyacrylamide gel electrophoresis and transferred onto Amersham Hybond-ECL nitrocellulose membranes (GE Healthcare, Chalfont St. Giles, Buckinghamshire, UK). The nonspecific binding sites were blocked by incubation in 5% nonfat dry milk in Tris-buffered saline/0.1% Tween 20 (Sigma-Aldrich) for 1 h at room temperature. Membranes were then incubated overnight at 4°C in the blocking buffer with polyclonal anti-neuronal nitric-oxide synthase (nNOS) (1:1000; Santa Cruz Biotechnology, Santa Cruz, CA), anti-endothelial nitric-oxide synthase (eNOS) (1:1000; Santa Cruz Biotechnology), and monoclonal anti-β-actin (1:1000; Sigma-Aldrich). Membranes were washed with Tris-buffered saline/0.1% Tween 20 and incubated with the horseradish peroxidase-conjugated secondary antibodies (1:2000; GE Healthcare) for 1 h at room temperature in 5% nonfat dry milk. Immunoreactive bands were detected with the enhanced chemiluminescence reagent (GE Healthcare).

Statistical Analysis. All data were expressed as mean ± S.E.M. Statistical comparisons between treated experimental groups and controls were performed using the one-way analysis of variance, followed by the Newman-Keuls test. $P < 0.05$ was considered statistically significant.

Results

Pharmacological Regulation of DAF-2DA-Monitored NO Level in Stably Transfected BHK-NCX1, BHK-NCX2, and BHK-NCX3 Cells. Western blot analysis revealed that BHK wild-type (BHK-Wt) and BHK cells stably transfected with each of the NCX isoforms expressed eNOS, whereas the splicing variants of nNOS were not detected (Fig. 1A). In these cells, when the NOS substrate L-arginine

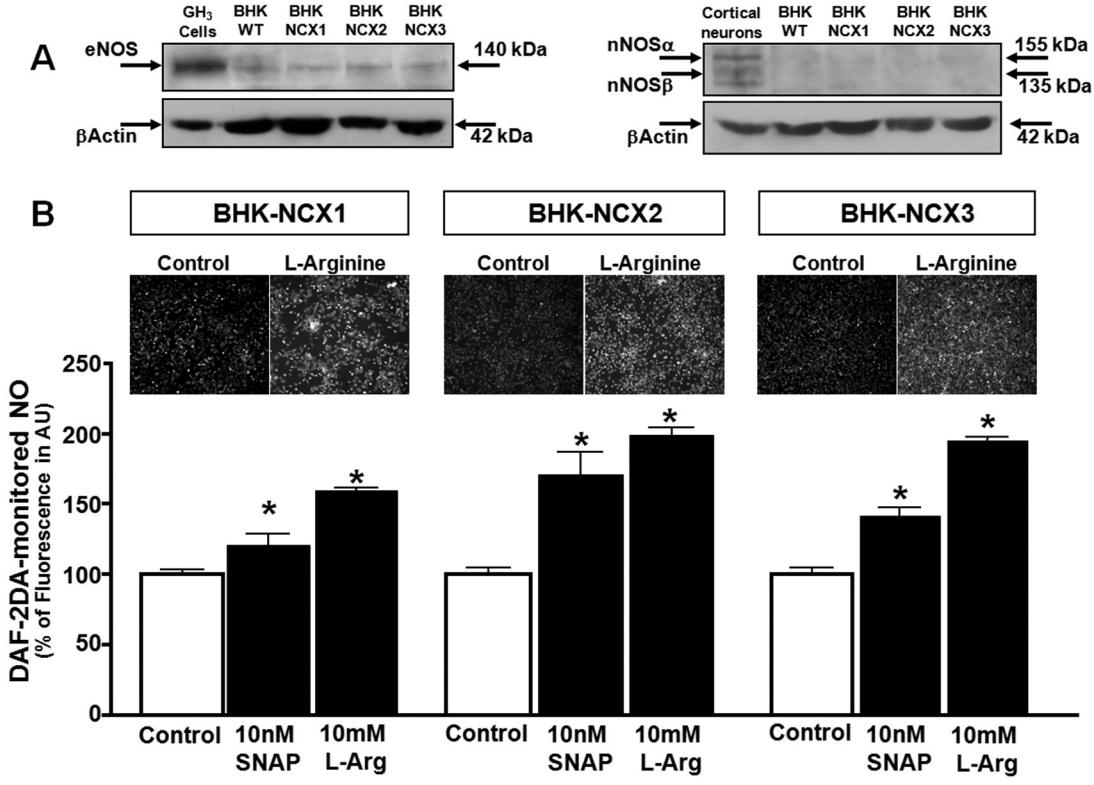

Fig. 1. Effect of the NO donor SNAP and the NO precursor L-arginine on DAF-2-monitored NO in stably transfected BHK-NCX1, BHK-NCX2, and BHK-NCX3 cells. A, representative Western blots of eNOS and nNOSα/nNOSβ expression in BHK-WT, BHK-NCX1, BHK-NCX2, and BHK-NCX3 cells. B, the insert depicts fluorescent images of DAF-2DA loaded BHK-NCX1 (left), BHK-NCX2 (middle), and BHK-NCX3 (right) cells under control conditions and after L-arginine treatment (10 mM/10 min). Bottom, bar graph of DAF-2-monitored NO measurements after 10-min incubation with SNAP (10 nM) or L-arginine (10 mM). Each bar represents the mean ± S.E.M. of three values obtained from different experimental sections. All data are reported as a percentage of control fluorescence expressed in arbitrary units. *, $P < 0.05$ versus each respective control group.

MOL PHARM
MOLECULAR PHARMACOLOGY
aspet
Downloaded from molpharm.aspetjournals.org by guest on December 1, 2012

(10 mM) was administered, an increase in DAF-2-monitored NO level was detected intracellularly (Fig. 1B). Likewise, the addition of the NO donor SNAP (10 nM) significantly increased intracellular DAF-2 fluorescence compared with respective untreated controls (Fig. 1B). Identical results were obtained in BHK-Wt exposed to L-arginine (10 mM) or SNAP (10 nM) (data not shown).

Effects of NO on NCX1, NCX2, and NCX3 Activity in BHK Cells Stably Transfected by Single-Cell Fura-2 Microfluorometry. The modulation exerted by NO on NCX1, NCX2, and NCX3 activity was studied in stably transfected BHK cells in the presence of the NO-donor SNAP or the NO precursor L-arginine by means of single-cell Fura-2 microfluorometry (Fig. 2). NCX activity was evaluated in the reverse mode of operation by monitoring $[Ca^{2+}]_i$ increases, elicited by an Na^+-deficient $NMDG^+$ (Na^+-free) medium, in the presence of the sarco(endo)plasmic reticulum Ca^{2+} ATPase inhibitor thapsigargin (1 μM). In BHK-NCX1 cells, the perfusion of Na^+-free was followed by an increase in $[Ca^{2+}]_i$ that was further increased by the NO donor SNAP (10 nM), thus displaying a significant enhancement of its activity in the reverse mode of operation (Fig. 2, A and B). Likewise, L-arginine (10 mM) reproduced the same stimulatory effect on NCX1 reverse mode (Fig. 2, A and B). The latter action was cGMP-independent because the guanylyl-cyclase inhibitor ODQ (100 nM) failed to prevent the NO-induced up-regulation of NCX1 activity (Fig. 2, A and B). No effect on $[Ca^{2+}]_i$ was recorded in BHK-Wt cells when perfused with Na^+-free (data not shown). As already observed for NCX1, in BHK-NCX2 cells, Na^+-free-induced $[Ca^{2+}]_i$ increases were significantly reinforced by SNAP (10 nM) (Fig. 2, C and D). Likewise, preincubation with the NO precursor L-arginine (10 mM) was able to reproduce the same

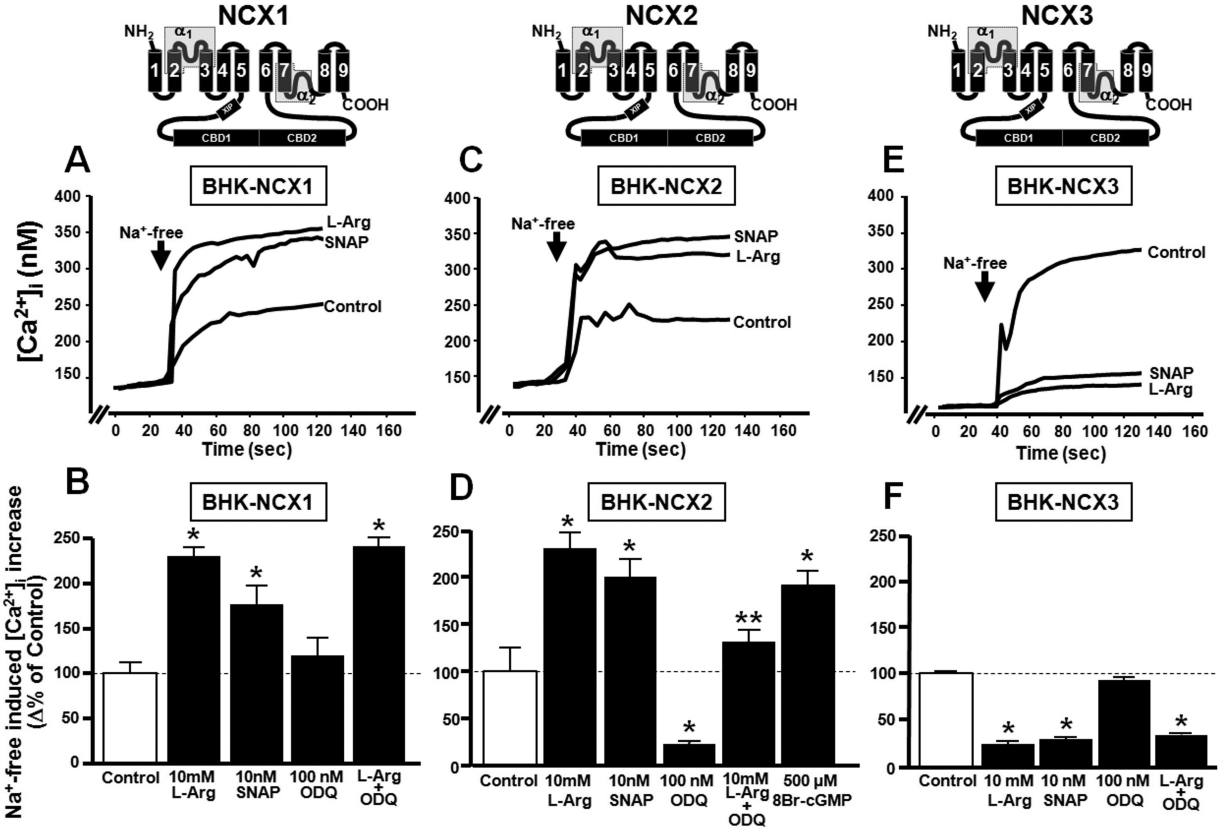

Fig. 2. Effect of the NO donor SNAP and of the NO precursor L-arginine on NCX1, NCX2, and NCX3 activity measured as Na^+-Free-induced $[Ca^{2+}]_i$ increase in stably transfected BHK-NCX1, BHK-NCX2, and BHK-NCX3 cells. A, superimposed single-cell traces representative of the effect of Na^+-Free on $[Ca^{2+}]_i$ on BHK-NCX1 cells when this solution was perfused alone or in the presence of SNAP (10 nM) or L-arginine (10 mM); both drugs were preincubated for 10 min. For each experiment, 40 to 65 individual cells were monitored. Top, NCX1 wild type. B, quantification of $[Ca^{2+}]_i$ increase induced by Na^+-Free in the presence of the following treatments: L-arginine (10 mM), SNAP (10 nM), ODQ (100 nM), and L-arginine + ODQ (10 mM + 100 nM, respectively), all preincubated for 10 min. $[Ca^{2+}]_i$ response to Na^+-free was calculated as the percentage change of increase of plateau values above baseline $[Ca^{2+}]_i$. Each bar represents the mean (± S.E.M.) of the aforementioned experimental values studied in three independent experimental sessions. *, $P < 0.05$ versus control values. C, superimposed single-cell traces representative of the effect of Na^+-Free on $[Ca^{2+}]_i$ in BHK-NCX2 cells when this solution was perfused alone or in the presence of SNAP (10 nM) or L-arginine (10 mM), both preincubated for 10 min. For each experiment, 40 to 65 individual cells were monitored. Top, NCX2 wild type. D, quantification of $[Ca^{2+}]_i$ increase induced by the Na^+-Free in the presence of the following treatments: L-arginine (10 mM), SNAP (10 nM), ODQ (100 nM), L-arginine + ODQ (10 mM + 100 nM, respectively), and 8-Br-cGMP (500 μM), all preincubated for 10 min. Each bar represents the mean (± S.E.M.) of the aforementioned experimental values studied in three independent experimental sessions. *, $P < 0.05$ versus control values; **, $P < 0.05$ versus L-arginine. E, superimposed single-cell traces representative of the effect of Na^+-Free on $[Ca^{2+}]_i$ in BHK-NCX3 cells when this solution was perfused alone or in the presence of SNAP (10 nM) or L-arginine (10 mM); both treatments were preincubated for 10 min. For each experiment, 40 to 65 individual cells were monitored. Top, NCX3 wild type. F, quantification of $[Ca^{2+}]_i$ increase induced by Na^+-Free in the presence of the following treatments: L-arginine (10 mM), SNAP (10 nM), ODQ (100 nM), and L-arginine + ODQ (10 mM + 100 nM, respectively), all preincubated for 10 min. Each bar represents the mean (± S.E.M.) of the aforementioned experimental values studied in three independent experimental sessions. *, $P < 0.05$ versus control and ODQ groups. In control conditions, the percentage of $[Ca^{2+}]_i$ increase after Na^+-free perfusion was 37.66 ± 4.2 for NCX1, 30.7 ± 1.06 for NCX2, and 37.03 ± 7.28 for NCX3. These data are calculated as the percentage change of plateau/basal $[Ca^{2+}]_i$ values.

MOL PHARM
MOLECULAR PHARMACOLOGY
aspet
Downloaded from molpharm.aspetjournals.org by guest on December 1, 2012

stimulatory effect exerted by SNAP on NCX2 reverse mode of operation (Fig. 2, C and D). However, unlike BHK-NCX1 cells, this increase was cGMP-dependent because the guanylyl-cyclase inhibitor ODQ (100 nM) not only reduced its basal activity but also prevented NO-induced increases in NCX2 activity operating in the reverse mode (Fig. 2D). To confirm the role of cGMP in NO-mediated NCX2 stimulation, the effect of its cell-permeable analog 8-Br-cGMP (500 μM) was studied in BHK-NCX2 cells. As expected, it reproduced the same stimulatory effect exerted by NO on Na^+-free-induced NCX2 activity (Fig. 2D). Unlike the stimulatory effect of NO on the activity of NCX1 and NCX2, single-cell Fura-2 experiments revealed that the NO donor SNAP (10 nM) significantly reduced NCX3 reverse mode of operation (Fig. 2, E and F). Likewise, preincubation with the NOS substrate L-arginine (10 mM) reproduced the same inhibitory effect (Fig. 2, E and F). Furthermore, NO effect on NCX3 was cGMP-independent because the guanylyl-cyclase inhibitor ODQ (100 nM) failed to counteract this inhibition (Fig. 2F).

Effects of NO on I_{NCX1}, I_{NCX2}, and I_{NCX3} Measured in Stably Transfected BHK Cells by Patch Clamp in Whole-Cell Configuration. To further characterize the differential roles exerted by NO on the activity of the NCX isoforms, patch-clamp recordings in whole-cell configuration were performed. Electrophysiological studies on BHK-NCX1 and BHK-NCX2 cells revealed that NO donor SNAP (10 nM) and L-arginine (10 nM) were able to enhance I_{NCX1} (Fig. 3, A and B) and I_{NCX2} (Fig. 3, C and D) either in the forward or reverse mode of operation. By contrast, experiments on BHK-NCX3 cells showed that both NO-donor SNAP (10 nM) and L-arginine (10 mM) inhibited I_{NCX3} in the reverse and forward modes of operation compared with control currents (Fig. 3, E and F).

Effects of NO on the Activity NCX1, NCX2, and NCX3 Mutants and Chimeras in Stably Transfected BHK Cells. To investigate the molecular determinants of NO on the molecular structure of each NCX isoform, the intracellular f-loop, a region mainly involved in the regulation of NCX function, was deleted in NCX1, NCX2, and NCX3 cDNAs. In particular, the effect of the gaseous mediator was investigated in NCX1Δ241–680, NCX2Δ269–662, and NCX3Δ292–708 mutants lacking the f-loop and named NCX1,2,3Δf (Fig. 4). Fura-2/AM single-cell video-imaging and patch-clamp experiments revealed that the elimination of the f-loop

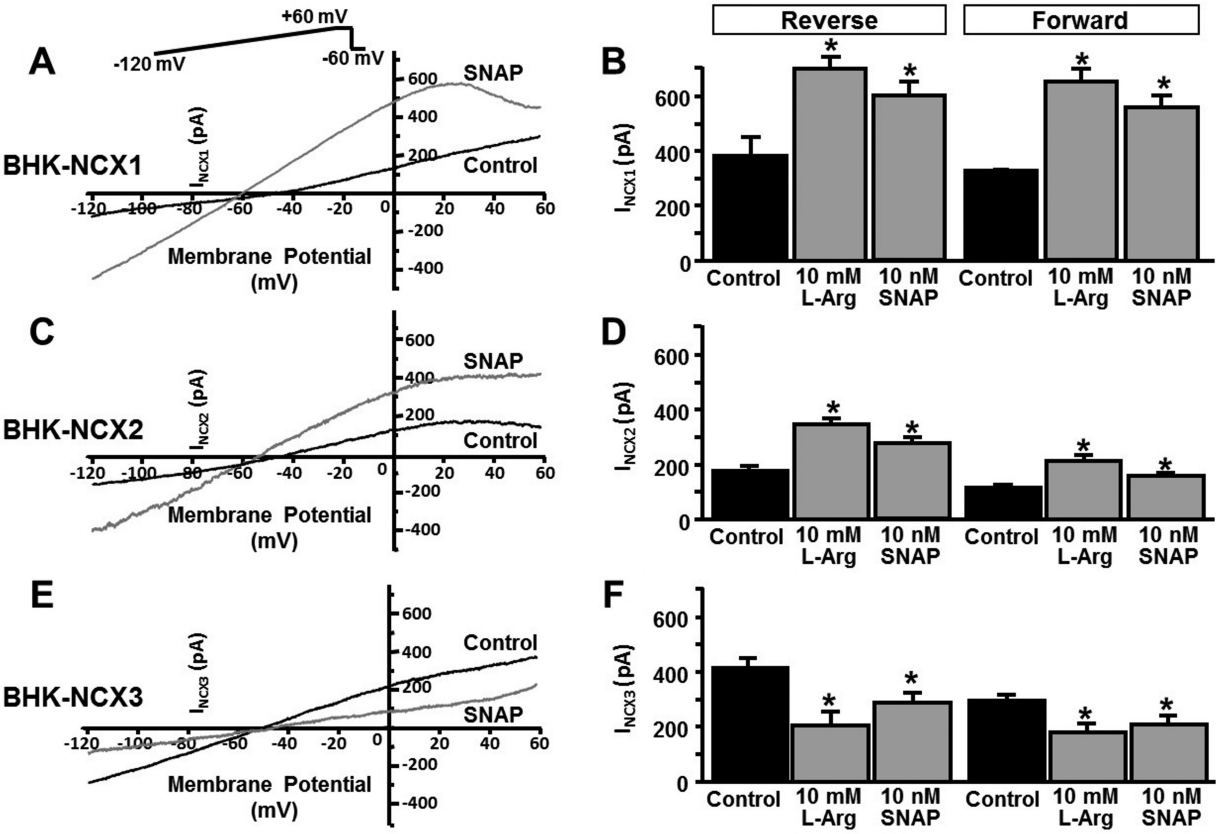

Fig. 3. Effect of the NO donor SNAP and the NO precursor L-arginine on I_{NCX1}, I_{NCX2}, and I_{NCX3} evaluated both in the reverse and in the forward modes of operation by means of patch-clamp in stably transfected BHK cells. A, I_{NCX} superimposed traces recorded from BHK-NCX1 cells under control conditions (black trace) and after 10 min preincubation with SNAP (10 nM) (gray trace). The electrophysiological protocol is reported at the top. B, I_{NCX1} quantification of the reverse mode at +10 mV and of the forward mode at −120 mV under control conditions and after 10-min preincubation with either L-arginine (10 mM) or SNAP (10 nM). The values are expressed as mean ± S.E.M. of current densities recorded from 20 cells in each experimental group obtained from three independent experimental sessions. *, $P < 0.05$ versus each respective control. C, I_{NCX} superimposed traces recorded from BHK-NCX2 cells under control conditions (black trace) and after 10-min preincubation with SNAP (10 nM) (gray trace). D, I_{NCX2} quantification of the reverse mode at +60 mV and the forward mode at −120 mV under control conditions and after 10-min preincubation with L-arginine (10 mM) or SNAP (10 nM). The values are expressed as mean ± S.E.M. of current densities recorded from 30 cells in each experimental group obtained from three independent experimental sessions. *, $P < 0.05$ versus each respective control. E, I_{NCX} superimposed traces recorded from BHK-NCX3 cells under control conditions (black trace) and after 10-min preincubation with SNAP (10 nM) (gray trace). F, I_{NCX3} quantification of the reverse mode at +60 mV and of the forward mode at −120 mV under control conditions and after 10-min preincubation with L-arginine (10 mM) or SNAP (10 nM). The values are expressed as mean ± S.E.M. of current densities recorded from 20 cells in each experimental group obtained from three independent experimental sessions. *, $P < 0.05$ versus each respective control.

MOL PHARM
MOLECULAR PHARMACOLOGY
aspet
Downloaded from molpharm.aspetjournals.org by guest on December 1, 2012

MOL PHARM

MOLECULAR PHARMACOLOGY

produced a significant change in the action profile exerted by NO on NCX1 and NCX2 activity. In fact, the removal of the f-loop not only abolished the stimulatory effect of SNAP (10 nM) observed in NCX1 and NCX2 wild-type isoforms but also converted NO stimulation into an inhibition of NCX1Δf and NCX2Δf mutant activity, both in the reverse and in the forward modes of operation (Fig. 4, A, B, and C). L-Arginine (10 mM) reproduced the same effect exerted by the NO-donor on each cellular clone (data not shown).

In contrast, the removal of the f-loop did not prevent the inhibitory action of SNAP (10 nM) on NCX3 either in the reverse or in the forward mode of operation (Fig. 4, A, B, and C), suggesting the existence of an inhibitory site located outside this region. Moreover, to better characterize the portion of the NCX1 and NCX2 f-loop involved in NO stimulatory action, we generated two NCX1 mutants lacking the 246 to 321 (NCX1Δ246–321) and 723 to 734 (NCX1Δ723–734) segments, respectively. The deletion of the 246 to 321 sequence from the NCX1 f-loop did not prevent the boosting effect of the NO-donor on its activity, as recorded in the reverse mode of operation by patch-clamp and Fura-2 microfluorometry (Fig. 5, B and E). However, the NO donor did not affect the forward mode of operation of NCX1Δ246–321 (Fig. 5, B and E). On the other hand, the deletion of the 723 to 734 sequence, a region with a lower percentage of identity with the sequence of the other two NCX isoforms (see alignment of Fig. 5) prevented the NO-stimulatory effect on NCX1 activity (Fig. 5, C and E). Indeed, SNAP (10 nM) was able to inhibit rather than potentiate the activity of NCX1Δ723–734 both in the reverse and in the forward modes of operation, as recorded by patch-clamp and Fura-2 microfluorometry (Fig. 5, C and E). Moreover, the single substitution of the Cys730 with a serine within this portion in NCX1C730S mutant was sufficient to reproduce SNAP inhibitory effect observed in NCX1Δ723–734 (Fig. 5, D and E). L-Arginine (10 mM) reproduced the same effect exerted by the NO-donor on each of these NCX1 mutants (data not shown).

Regarding NCX2, deletion mutagenesis revealed that the elimination of the f-loop portion 669 to 744 (NCX2Δ669–744) but not of the 275 to 348 region (NCX2Δ275–348) prevented the NO-mediated stimulatory effect (Fig. 6, B, C, and E). In fact, SNAP (10 nM) inhibited rather than potentiated the activity of NCX2Δ669–744 mutant both in the reverse and in the forward modes of operation, as recorded by patch-clamp and Fura-2 microfluorometry (Fig. 6, C and E). It is noteworthy that the substitution of the four amino acids DGSR in the

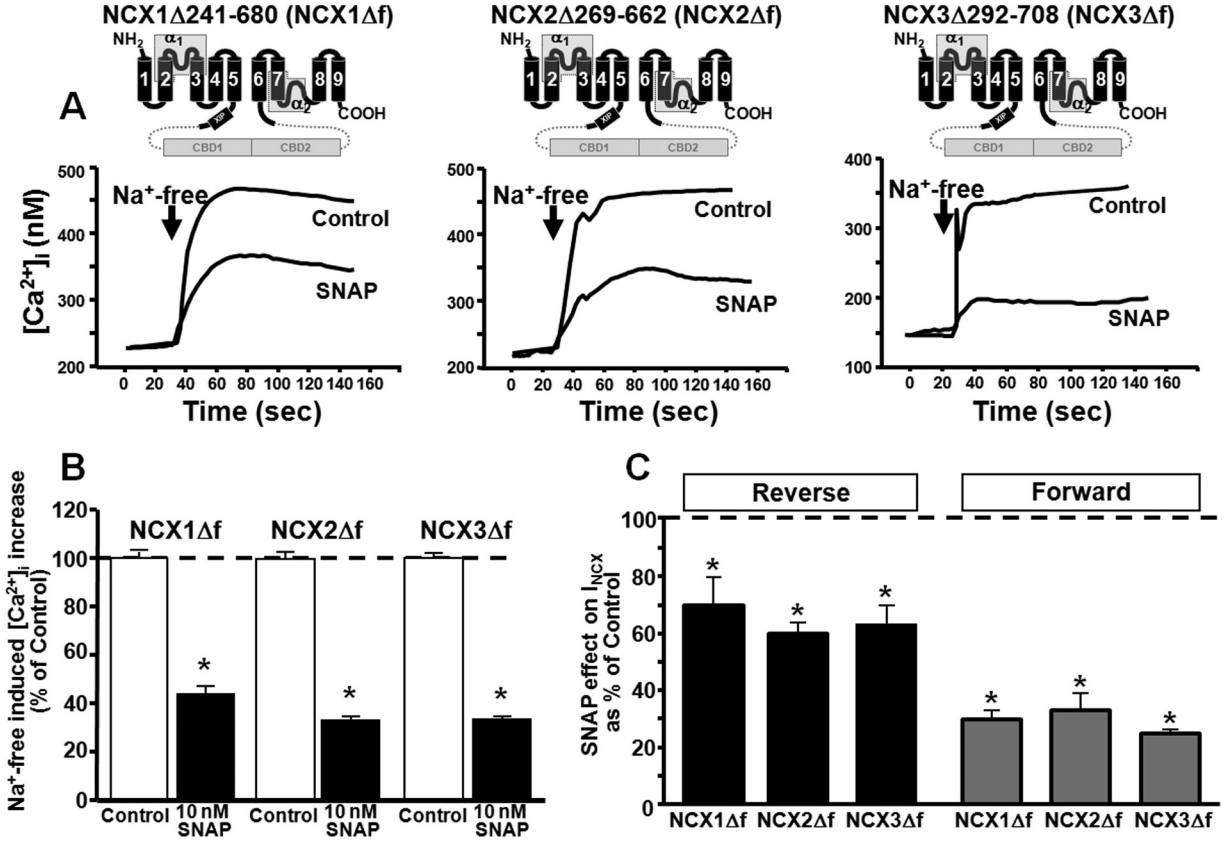

Fig. 4. Effect of the NO donor SNAP on the activity of NCX1Δf, NCX2Δf, and NCX3Δf mutants stably transfected in BHK cells measured by Fura-2 microfluorometry and patch clamp. A, superimposed single-cell traces representative of the effect of Na^+-Free on $[Ca^{2+}]_i$ when this solution was perfused alone or in the presence of SNAP (10 nM) in NCX1Δf (left), NCX2Δf (middle), and NCX3Δf (right) mutants, depicted at the top. The percentage of $[Ca^{2+}]_i$ increase after Na^+-free perfusion, calculated as the percentage change of plateau/basal value, was 50.5 ± 1.7 for NCX1Δf (∗, $P <$ 0.05 versus NCX1 Wt), 66.9 ± 1.3 for NCX2Δf (∗$P < 0.05$ versus NCX2 Wt), and 34.25 ± 5.37 for NCX3Δf. For each experiment, 50 to 65 individual cells were monitored. B, quantification of the effect of SNAP (10 nM) on $[Ca^{2+}]_i$ increase induced by the Na^+-Free in the aforementioned Δf mutants. Each bar represents the mean (± S.E.M.) of the values obtained from three independent experimental sessions. ∗, $P < 0.05$ versus respective controls. C, quantification of the effect of SNAP (10 nM) on I_{NCX} reverse and forward modes of operation recorded in BHK-NCX1Δf, BHK-NCX2Δf, and BHK-NCX3Δf mutants. The values are expressed as mean ± S.E.M. of current densities recorded in approximately 10 cells in each experimental group obtained from three independent experimental sessions. For the quantification of the experiments, the activity of the corresponding controls (wild type) was considered as 100%. ∗, $P < 0.05$ versus respective controls.

Downloaded from molpharm.aspetjournals.org by guest on December 1, 2012

711-to-714 sequence of NCX2 with the two amino acids SG present in the corresponding NCX3 region was sufficient to prevent the NO-mediated stimulatory effect on NCX2 activity (Fig. 6, D and E). Indeed, patch-clamp and Fura-2/AM data evidenced that SNAP (10 nM) inhibited rather than potentiated the activity of this mutant named NCX2SG (Fig. 6, D and E). L-Arginine (10 mM) reproduced the same effect exerted by the NO-donor on each NCX2 mutant (data not shown).

To establish the site responsible for NO-mediated down-regulation of NCX3 activity, we performed a site-directed mutagenesis of the Cys156 in the α1 repeat sequence, a site potentially involved in NO inhibitory modulation. Actually, the substitution of Cys156 with a serine (NCX3C156S) prevented the NO-mediated inhibition of NCX3 activity in the reverse and forward modes of operation, as revealed by patch-clamp and Fura-2 microfluorometry (Fig. 7, B and E). These data were also reproduced by the NO-precursor L-arginine (10 mM) (data not shown).

To further support the data obtained by deletion and site-directed mutagenesis on NO determinants present on each NCX isoform, we generated two chimeras between NCX3 and NCX1 or NCX3 and NCX2, respectively. In particular, we substituted the NO-insensitive NCX3 region 707 to 776 with the homologous NO-sensitive NCX1 segment 718 to 787, thus producing the chimera named $NCX3_{NCX1TM6\text{-}floop}$ (Fig. 7C). It is noteworthy that the activity of this $NCX3_{NCX1TM6\text{-}floop}$ chimera was potentiated by SNAP (10 nM) in both the reverse and the forward modes of operation, as recorded by patch-clamp and Fura-2 microfluorometry (Fig. 7, C and E). Furthermore, a chimera between NCX3 and NCX2, named $NCX3_{NCX2DGSR}$,was produced by introducing in the NO-insensitive NCX3 region 719 to 720 the homologous NO-sensitive NCX2 sequence 711 to 714 (Fig. 7D). Patch-clamp and Fura-2 microfluorometry recordings

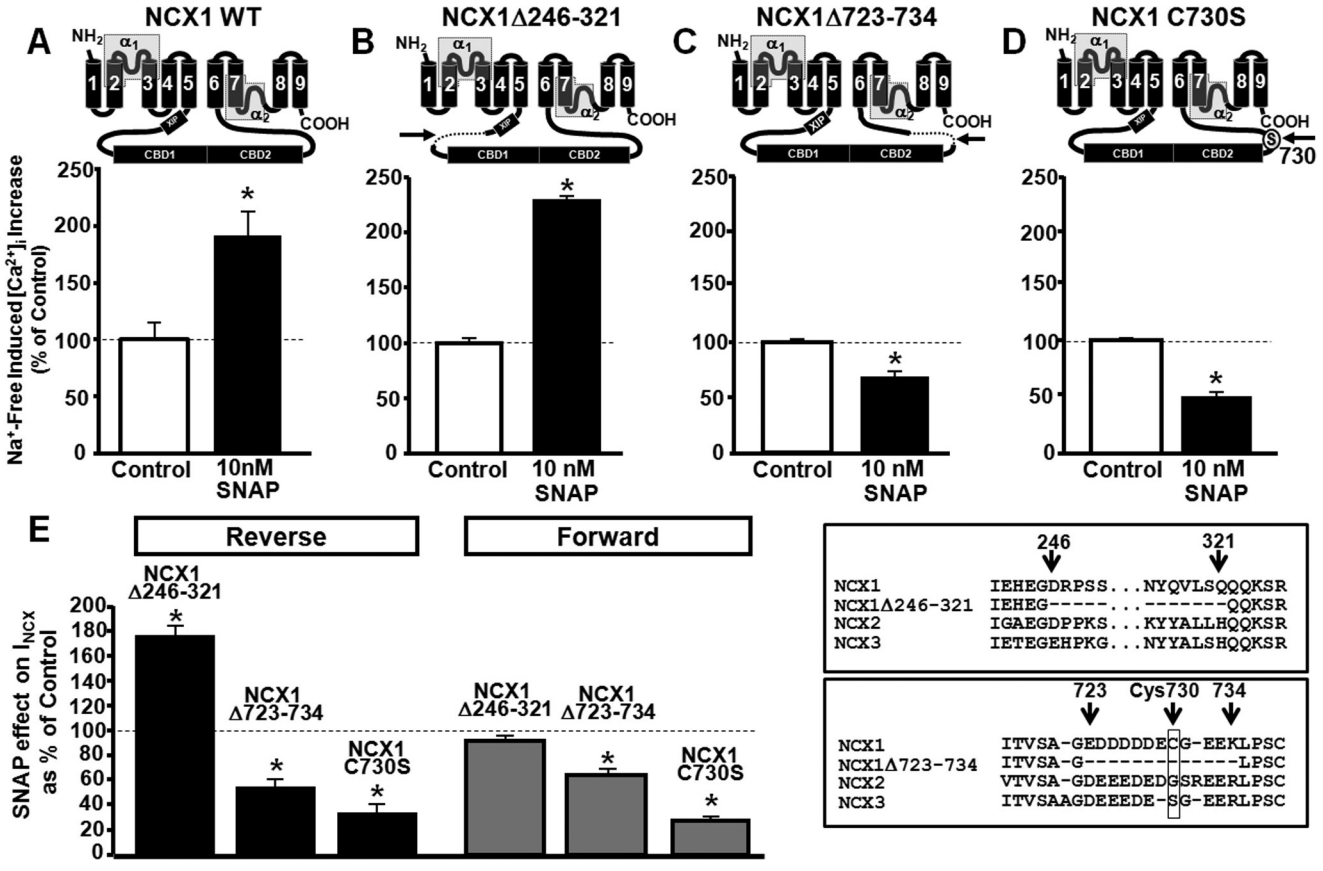

Fig. 5. Effect of the NO donor SNAP on the activity of NCX1Δ246–321, NCX1Δ723–734, and NCX1C730S mutants stably transfected in BHK cells and measured by means of Fura-2 microfluorometry and patch-clamp. A, quantification of the effect of SNAP (10 nM) on $[Ca^{2+}]_i$ increase induced by Na^+-Free in BHK-NCX1 Wt, depicted at the top. Each bar represents the mean (± S.E.M.) of the values obtained in three independent experimental sessions. For each experiment, 40 to 65 individual cells were monitored. *, $P < 0.05$ versus control. B, quantification of the effect of SNAP (10 nM) on $[Ca^{2+}]_i$ increase induced by Na^+-Free in NCX1Δ246–321 mutant, depicted at the top. Each bar represents the mean (± S.E.M.) of the values obtained in three independent experimental sessions. For each experiment, 50 to 65 individual cells were monitored. *, $P < 0.05$ versus its internal control. C, quantification of the effect of SNAP (10 nM) on $[Ca^{2+}]_i$ increase induced by Na^+-Free in NCX1Δ723–734 mutant, depicted at the top. Each bar represents the mean (± S.E.M.) of the values obtained in three independent experimental sessions. For each experiment, 50 to 65 individual cells were monitored. *, $P < 0.05$ versus its control. D, quantification of the effect of SNAP (10 nM) on $[Ca^{2+}]_i$ increase induced by Na^+-Free in NCX1C730S mutant, depicted at the top. Each bar represents the mean (± S.E.M.) of the values obtained in three independent experimental sessions. For each experiment, 50 to 65 individual cells were monitored. *, $P < 0.05$ versus its control. The percentage of $[Ca^{2+}]_i$ increase after Na^+-free perfusion, calculated as the percentage change of plateau/basal value, was 14.7 ± 1.6 for NCX1Δ246–321 (*, $P < 0.05$ versus NCX1 Wt), 35.7 ± 1.5 for NCX1Δ723–734, and 31.72 ± 1.48 for NCX1C730S. E, quantification of the effect of SNAP (10 nM) on I_{NCX} reverse and forward modes measured in NCX1Δ246–321, NCX1Δ723–734, and NCX1C730S mutants by patch-clamp. The values are expressed as mean ± S.E.M. of current densities recorded in almost 10 cells in each experimental group obtained from three independent experimental sessions and reported as a percentage of control values. *, $P < 0.05$ versus its respective control. The bottom of the figure shows the alignment of the amino acid sequence of the regions of interest (indicated by the arrows) on NCX1, NCX1Δ246–321, NCX2, NCX3, and NCX1Δ723–734.

MOL PHARM
MOLECULAR PHARMACOLOGY
aspet
Downloaded from molpharm.aspetjournals.org by guest on December 1, 2012

showed that $NCX3_{NCX2DGSR}$ chimera activity was enhanced by SNAP (10 nM) (Fig. 7, D and E). L-Arginine (10 mM) reproduced the same effect exerted by the NO donor on each chimera (data not shown).

Discussion

The results of the present study demonstrated that the gaseous mediator NO up-regulates the activity of both NCX1 and NCX2 isoforms in a cGMP-independent and -dependent manner, respectively. By contrast, the gaseous mediator inhibits NCX3 activity in a cGMP-independent way. The molecular determinant of NO action on NCX1 was localized within the f-loop at the level of Cys730, whereas that of NCX2 was localized within the corresponding region of the same loop at the level of 711 to 714. It is noteworthy that the molecular determinant of NCX3 was found outside the f-loop at the level of the α1 repeat.

Regarding cGMP-independent stimulatory action of NO on NCX1, it should be emphasized that the molecular determinant was a cysteine, thus suggesting that NO might increase NCX1 activity by direct nitrosylation occurring in the f-loop (i.e., the main regulatory domain of this antiporter). Instead, the molecular determinant of the cGMP-dependent NO action on NCX2 was a segment containing a serine, an amino acid that in several proteins is phosphorylated by cGMP-dependent kinases (PKG) (Francis et al., 2010). It is noteworthy that the putative NCX2 phosphorylation site DGSR, found in the present study, displays some similarities with the canonic consensus sequence of PKG $(R/K_{-2-3})(X/K)(S/T)X$ (Glass and Krebs, 1982) but differs only for the amino acid position in P_{-2} (R/K_{-2-3}). However, it has been reported that although this amino acid is apparently not crucial for the phosphorylation of PKG, it does improve its affinity for the substrate. On the other hand, it cannot be excluded that PKG might

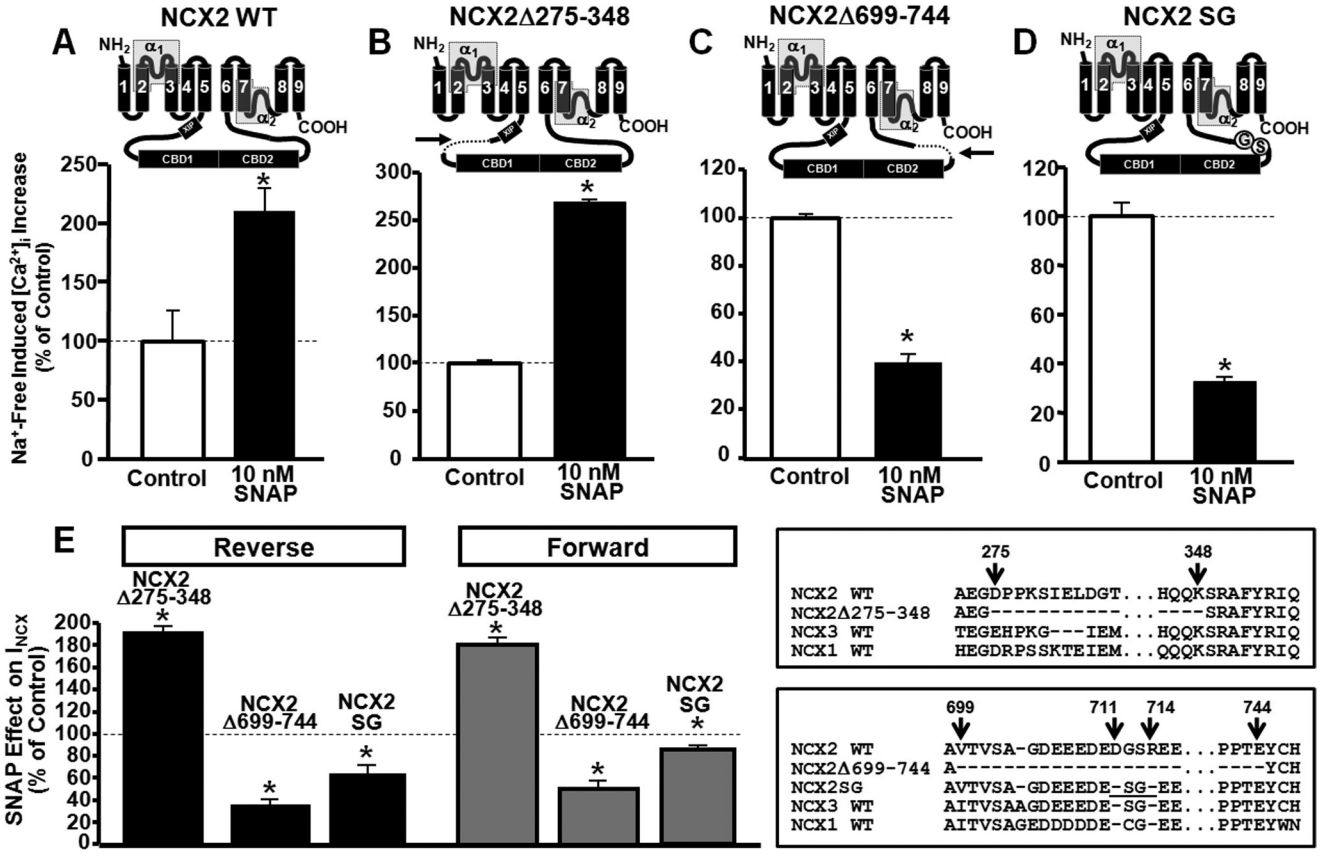

Fig. 6. Effect of the NO-donor SNAP on the activity of NCX2Δ275–348, NCX2Δ699–744, and NCX2SG mutants stably transfected in BHK cells and measured by Fura-2 microfluorometry and patch clamp. A, quantification of the effect of SNAP (10 nM) on $[Ca^{2+}]_i$ increase induced by Na^+-Free in BHK-NCX2 Wt, depicted at the top. Each bar represents the mean (± S.E.M.) of the values obtained in three independent experimental sessions. For each experiment, 40 to 65 individual cells were monitored. *, $P < 0.05$ versus its control. B, quantification of the effect of SNAP (10 nM) on $[Ca^{2+}]_i$ increase induced by Na^+-Free in NCX2Δ275–348 mutant, depicted at the top. Each bar represents the mean (± S.E.M.) of the values obtained in three independent experimental sessions. For each experiment, 50 to 65 individual cells were monitored. *, $P < 0.05$ versus its control. C, quantification of the effect of SNAP (10 nM) on $[Ca^{2+}]_i$ increase induced by Na^+-Free in NCX2Δ699–744 mutant, depicted at the top. Each bar represents the mean (± S.E.M.) of the values obtained in three independent experimental sessions. For each experiment, 40 to 65 individual cells were monitored. *, $P < 0.05$ versus its control. D, quantification of the effect of SNAP (10 nM) on $[Ca^{2+}]_i$ increase induced by Na^+-Free in NCX2SG mutant, depicted at the top. Each bar represents the mean (± S.E.M.) of the values obtained in three independent experimental sessions. For each experiment, 40 to 65 individual cells were monitored. *, $P < 0.05$ versus its control. The percentage of $[Ca^{2+}]_i$ increase after Na^+-free perfusion, calculated as the percentage change of plateau/basal value, was 11.17 ± 3 for NCX2Δ275–348 (*$P < 0.05$ versus NCX2 Wt), 33.55 ± 1.96 for NCX2Δ699–744, and 19.1 ± 5.7 for NCX2SG. E, quantification of the effect of SNAP (10 nM) on I_{NCX} reverse and forward modes measured in NCX2Δ275–348, NCX2Δ669–744, and NCX2SG mutants by patch clamp. The values are expressed as mean ± S.E.M. of current densities recorded in almost 10 cells in each experimental group obtained from three independent experimental sessions and reported as the percentage of control values. *, $P < 0.05$ versus respective controls. The bottom of the figure shows the alignment of the sequence of the regions of interest (indicated by the arrows) on NCX2, NCX2Δ275–348, NCX3, NCX1, NCX2Δ699–744, NCX2SG, and NCX1.

Downloaded from molpharm.aspetjournals.org by guest on December 1, 2012

exert its effect on the DGSR sequence of NCX2 through an indirect transductional mechanism.

Another peculiar aspect of NCX2 modulation was that in the absence of cGMP stimulation by the NO donor, inhibition of the guanylyl cyclase by ODQ reduced Na^+-free-evoked NCX2 activity, suggesting that basal levels of cGMP may also participate in the regulation of NCX2 activity. On the other hand, when ODQ is coincubated with L-arginine, the reduction in NCX2 activity does not reach the same level as that observed with ODQ alone. However, when ODQ exerts its inhibitory action on guanylyl-cyclase activity in the absence of L-arginine, cGMP levels are probably lower than those occurring in the presence of L-arginine. On the other hand, the possibility that L-arginine could exert a stimulatory effect on NCX2 through a cGMP-independent mechanism can not be ruled out.

Regarding cGMP-independent inhibition of NO on NCX3, all NCX mutants lacking the f loop (NCX1Δf, NCX2Δf, and NCX3Δf) were affected in the same way. This suggested that the putative nitrosylation site is located outside of this regulatory domain and is highly conserved among the NCX isoforms (Ottolia et al., 2005). It is noteworthy that the mutation of the highly conserved Cys156, located at the level of the α_1 repeat, prevented the NO-mediated inhibition of NCX3. Likewise, we could hypothesize that the homologous cysteine present in NCX1 and NCX2 may represent the molecular determinant of NCX1Δf and NCX2Δf inhibition by NO.

In addition, the participation of NO in the stimulation of NCX1 and NCX2 sequences 718 to 787 and 711 to 714, respectively, was further highlighted by NCX1/NCX2/NCX3 chimeras. In particular, when NCX3 chimeras were generated by replacing the NO-insensitive region with the homologous NO-sensitive segments of NCX1 or NCX2, the inhibitory action of NO on NCX3 activity was converted into a stimulatory one. Another intriguing finding emerging from the NCX1 and NCX2 mutants lacking the f-loop was that these two isoforms, in addition to having stimulatory molecular determinants, were also provided with a second site

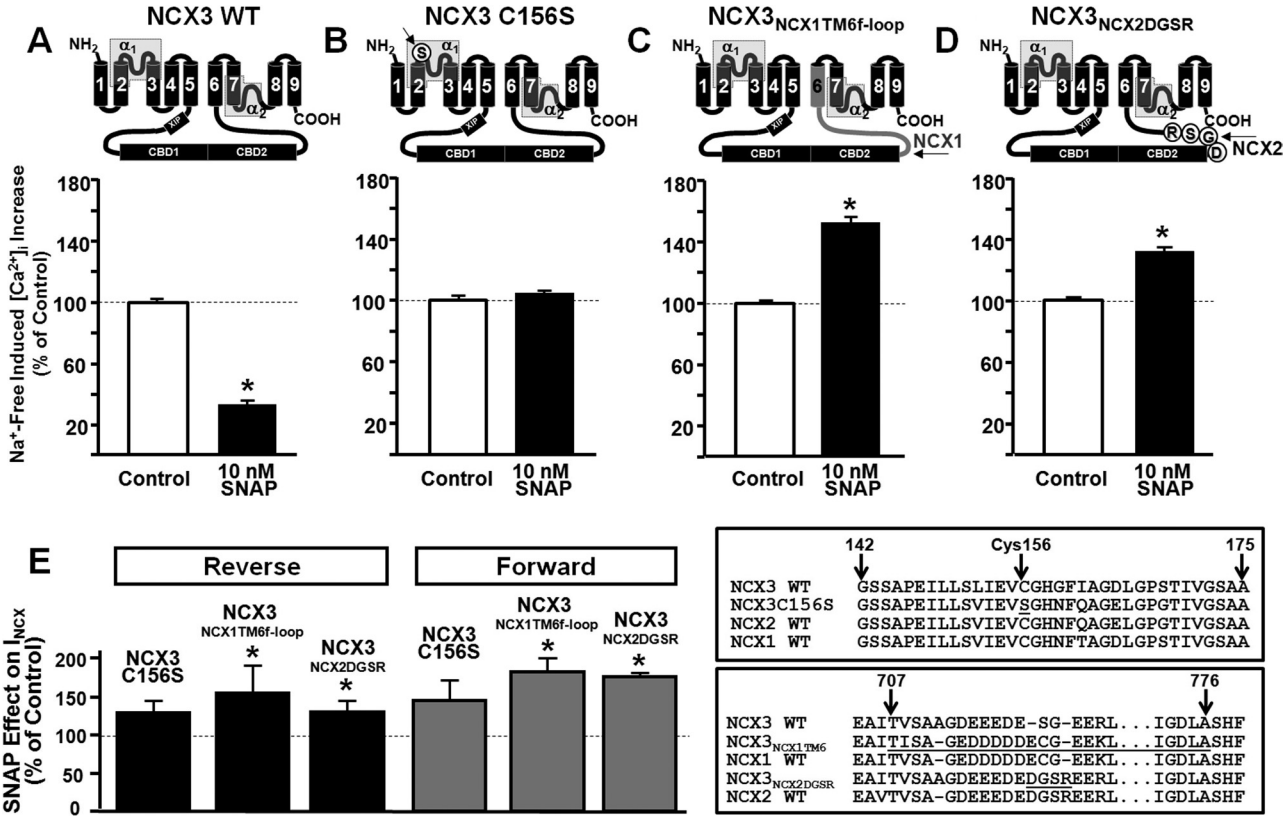

Fig. 7. Effect of the NO donor SNAP on the activity of NCX3C156S mutant $NCX3_{NCX1TM6\text{-}floop}$ and $NCX3_{NCX2DGSR}$ chimeras stably transfected in BHK cells and measured by Fura-2 microfluorometry and patch clamp. A, quantification of the effect of SNAP (10 nM) on $[Ca^{2+}]_i$ increase induced by Na^+-Free in NCX3 Wt, depicted at the top. Each bar represents the mean (± S.E.M.) of the values obtained in three independent experimental sessions. For each experiment, 40 to 65 individual cells were monitored. *, $P < 0.05$ versus its control. B, quantification of the effect of SNAP (10 nM) on $[Ca^{2+}]_i$ increase induced by Na^+-Free in NCX3C156S, depicted at the top. Each bar represents the mean (± S.E.M.) of the values obtained in three independent experimental sessions. For each experiment, 50 to 60 individual cells were monitored. *, $P < 0.05$ versus its control. Each bar represents the mean (± S.E.M.) of the values obtained in three independent experimental sessions. C, quantification of the effect of SNAP (10 nM) on $[Ca^{2+}]_i$ increase induced by Na^+-Free in $NCX3_{NCX1TM6\text{-}floop}$, depicted at the top. Each bar represents the mean (± S.E.M.) of the values obtained in three independent experimental sessions. For each experiment, 40 to 65 individual cells were monitored. *, $P < 0.05$ versus its control. D, quantification of the effect of SNAP (10 nM) on $[Ca^{2+}]_i$ increase induced by Na^+-Free in $NCX3_{DGSR}$, depicted at the top. Each bar represents the mean (± S.E.M.) of the values obtained in three independent experimental sessions. For each experiment, 50 to 65 individual cells were monitored. *, $P < 0.05$ versus its control. The percentage of $[Ca^{2+}]_i$ increase after Na^+-free perfusion, calculated as the percentage change of plateau/basal value, was 28.8 ± 3.2 for NCX3C156S, 36.48 ± 2.2 for $NCX3_{NCX1TM6\text{-}floop}$, and 48.25 ± 1.7 for $NCX3_{NCX2DGSR}$. E, quantification of the effect of SNAP (10 nM) on I_{NCX} reverse and forward modes measured in $NCX3_{NCX1TM6\text{-}floop}$ and $NCX3_{NCX2DGSR}$ chimeras and NCX3C156S mutant by patch clamp. The values are expressed as mean ± S.E.M. of current densities recorded in almost 10 cells in each experimental group obtained from three independent experimental sessions and reported as percentage of control values. *, $P < 0.05$ versus respective controls. The bottom of the figure shows the alignment of the sequence of the regions of interest (indicated by the arrows) on NCX3, NCX3C156S, NCX2, NCX1, $NCX3_{NCX1TM6\text{-}floop}$, and $NCX3_{NCX2DGSR}$.

Downloaded from molpharm.aspetjournals.org by guest on December 1, 2012

outside of the hydrophilic f-loop that mediated an NO-inhibitory action. However, despite the presence of this outer site, the effect of NO on the stimulatory sites prevailed. Although a definitive explanation for the role of this inhibitory site is still lacking, we could advance the hypothesis that the presence of this molecular determinant might become prevalent when changes in transductional factors—elicited by some pathophysiological conditions—turn off the stimulatory site. In previous studies, Asano et al. (1995) reported that cGMP and NO donors enhanced NCX activity in cultured rat astrocytes and cortical brain slices. However, they were unable to characterize the single contribution of each NCX isoform to this stimulatory action. This was probably because of the fact that when the three NCX isoforms are coexpressed in the same cells, the inhibitory effect of NO on NCX3 might be masked by the stimulatory action of the gaseous mediator on NCX1 and NCX2 isoforms.

In this regard, our study has provided several meaningful and insightful findings on the effect of NO on the modulation of the three NCX isoforms. First, NO can either stimulate or inhibit NCX isoforms. Second, it can selectively modulate each NCX isoform by acting on different molecular determinants that are specific for each isoform. Finally, it can exert its effect through different biochemical mechanisms. More specifically, the close interaction between NO and the three isoforms might indeed have biological relevance, because it occurs with several other intracellular factors including reactive oxygen species, $[H^+]_i$, ATP, $[Na^+]_i$, and $[Ca^{2+}]_i$ (Sanchez-Armass and Blaustein, 1987; Annunziato et al., 2004). For instance, NO production does undergo critical changes under physiological or pathophysiological conditions such as anoxia, oxidative stress, and neurodegenerative diseases (Annunziato et al., 2002) in which each NCX isoform plays a specific role (Boscia et al., 2006; Secondo et al., 2007; Sirabella et al., 2009).

Together, this study indicates that the gaseous mediator NO differently regulates NCX1, NCX2, and NCX3 activity. In particular, it stimulates NCX1 and NCX2 activity in cGMP-independent and cGMP-dependent manner, respectively. In addition, the molecular determinants of NO on NCX1 and NCX2 are localized in the same regulatory region of the f-loop, although it is differently modulated. In contrast, NO inhibits NCX3 activity, and, unlike the other sites, its molecular determinant is localized outside of the f-loop, at the level of the α1 repeat.

Acknowledgments

We thank Dr. Paola Merolla for the editorial revision and Vincenzo Grillo and Carmine Capitale for technical assistance.

Authorship Contributions

Participated in research design: Secondo, Molinaro, and Pannaccione.

Conducted experiments: Secondo, Molinaro, Pannaccione, Esposito, Cantile, Lippiello, and Sirabella.

Contributed new reagents or analytic tools: Iwamoto.

Performed data analysis: Secondo, Molinaro, and Pannaccione.

Wrote or contributed to the writing of the manuscript: Secondo, Molinaro, Pannaccione, Di Renzo, and Annunziato.

References

Annunziato L, Pannaccione A, Cataldi M, Secondo A, Castaldo P, Di Renzo G, and Taglialatela M (2002) Modulation of ion channels by reactive oxygen and nitrogen species: a pathophysiological role in brain aging? *Neurobiol Aging* **23:**819–834.

Annunziato L, Pignataro G, and Di Renzo GF (2004) Pharmacology of brain Na^+/Ca^{2+} exchanger: from molecular biology to therapeutic perspectives. *Pharmacol Rev* **56:**633–654.

Asano S, Matsuda T, Takuma K, Kim HS, Sato T, Nishikawa T, and Baba A (1995) Nitroprusside and cyclic GMP stimulate Na^+-Ca^{2+} exchange activity in neuronal preparations and cultured rat astrocytes. *J Neurochem* **64:**2437–2441.

Berridge MJ, Lipp P, and Bootman MD (2000) The versatility and universality of calcium signalling. *Nat Rev Mol Cell Biol* **1:**11–21.

Boscia F, Gala R, Pignataro G, de Bartolomeis A, Cicale M, Ambesi-Impiombato A, Di Renzo G, and Annunziato L (2006) Permanent focal brain ischemia induces isoform-dependent changes in the pattern of Na^+/Ca^{2+} exchanger gene expression in the ischemic core, periinfarct area, and intact brain regions. *J Cereb Blood Flow Metab* **26:**502–517.

Brakemeier S, Eichler I, Knorr A, Fassheber T, Köhler R, and Hoyer J (2003) Modulation of Ca^{2+}-activated K+ channel in renal artery endothelium in situ by nitric oxide and reactive oxygen species. *Kidney Int* **64:**199–207.

Formisano L, Saggese M, Secondo A, Sirabella R, Vito P, Valsecchi V, Molinaro P, Di Renzo G, and Annunziato L (2008) The two isoforms of the Na^+/Ca^{2+} exchanger, NCX1 and NCX3, constitute novel additional targets for the prosurvival action of Akt/protein kinase B pathway. *Mol Pharmacol* **73:**727–737.

Francis SH, Busch JL, Corbin JD, and Sibley D (2010) cGMP-dependent protein kinases and cGMP phosphodiesterases in nitric oxide and cGMP action. *Pharmacol Rev* **62:**525–563.

Furukawa K, Ohshima N, Tawada-Iwata Y, and Shigekawa M (1991) Cyclic GMP stimulates Na^+/Ca^{2+} exchange in vascular smooth muscle cells in primary culture. *J Biol Chem* **266:**12337–12341.

Glass DB and Krebs EG (1982) Phosphorylation by guanosine 3′:5′-monophosphate-dependent protein kinase of synthetic peptide analogs of a site phosphorylated in histone H2B. *J Biol Chem* **257:**1196–1200.

Grynkiewicz G, Poenie M, and Tsien RY (1985) A new generation of Ca^{2+} indicators with greatly improved fluorescence properties. *J Biol Chem* **260:**3440–3450.

He LP, Cleemann L, Soldatov NM, and Morad M (2003) Molecular determinants of cAMP-mediated regulation of the Na^+-Ca^{2+} exchanger expressed in human cell lines. *J Physiol* **548:**677–689.

Inglese M, Madelin G, Oesingmann N, Babb JS, Wu W, Stoeckel B, Herbert J, and Johnson G (2010) Brain tissue sodium concentration in multiple sclerosis: a sodium imaging study at 3 tesla. *Brain* **133:**847–857.

Iwamoto T, Pan Y, Nakamura TY, Wakabayashi S, and Shigekawa M (1998) Protein kinase C-dependent regulation of Na^+/Ca^{2+} exchanger isoforms NCX1 and NCX3 does not require their direct phosphorylation. *Biochemistry* **37:**17230–17238.

Lee SL, Yu AS, and Lytton J (1994) Tissue-specific expression of Na^+-Ca^{2+} exchanger isoforms. *J Biol Chem* **269:**14849–14852.

Li Z, Matsuoka S, Hryshko LV, Nicoll DA, Bersohn MM, Burke EP, Lifton RP, and Philipson KD (1994) Cloning of the NCX2 isoform of the plasma membrane Na^+-Ca^{2+} exchanger. *J Biol Chem* **269:**17434–17439.

Melisi D, Secondo A, Montoro P, Piacente S, Rimoli MG, Minale M, de Caprariis P, and Annunziato L (2006) Galactosyl derivatives of L-arginine and D-arginine: synthesis, stability, cell permeation, and nitric oxide production in pituitary GH3 cells. *J Med Chem* **49:**4826–4833.

Molinaro P, Cuomo O, Pignataro G, Boscia F, Sirabella R, Pannaccione A, Secondo A, Scorziello A, Adornetto A, Gala R, et al. (2008) Targeted disruption of Na^+/Ca^{2+} exchanger 3 (NCX3) gene leads to a worsening of ischemic brain damage. *J Neurosci* **28:**1179–1184.

Nagano T, Kawasaki Y, Baba A, Takemura M, and Matsuda T (2004) Up-regulation of Na^+-Ca^{2+} exchange activity by interferon-gamma in cultured rat microglia. *J Neurochem* **90:**784–791.

Nicoll DA, Longoni S, and Philipson KD (1990) Molecular cloning and functional expression of the cardiac sarcolemmal Na^+-Ca^{2+} exchanger. *Science* **250:**562–565.

Nicoll DA, Quednau BD, Qui Z, Xia YR, Lusis AJ, and Philipson KD (1996) Cloning of a third mammalian Na^+-Ca^{2+} exchanger, NCX3. *J Biol Chem* **271:**24914–24921.

Ottolia M, Nicoll DA, and Philipson KD (2005) Mutational analysis of the alpha-1 repeat of the cardiac Na^+-Ca^{2+} exchanger. *J Biol Chem* **280:**1061–1069.

Papa M, Canitano A, Boscia F, Castaldo P, Sellitti S, Porzig H, Taglialatela M, and Annunziato L (2003) Differential expression of the Na^+-Ca^{2+} exchanger transcripts and proteins in rat brain regions. *J Comp Neurol* **461:**31–48.

Peers C, Smith IF, Boyle JP, and Pearson HA (2004) Remodelling of Ca^{2+} homeostasis in type I cortical astrocytes by hypoxia: evidence for association with Alzheimer's disease. *Biol Chem* **385:**285–289.

Pignataro G, Gala R, Cuomo O, Tortiglione A, Giaccio L, Castaldo P, Sirabella R, Matrone C, Canitano A, Amoroso S, Di Renzo G, and Annunziato L (2004) Two sodium/calcium exchanger gene products, NCX1 and NCX3, play a major role in the development of permanent focal cerebral ischemia. *Stroke* **35:**2566–2570.

Sanchez-Armass S and Blaustein MP (1987) Role of sodium-calcium exchange in regulation of intracellular calcium in nerve terminals. *Am J Physiol* **252:**C595–C603.

Secondo A, Pannaccione A, Cataldi M, Sirabella R, Formisano L, Di Renzo G, and Annunziato L (2006) Nitric oxide induces $[Ca^{2+}]$i oscillations in pituitary GH3 cells: involvement of IDR and ERG K+ currents. *Am J Physiol Cell Physiol* **290:**C233–C243.

Secondo A, Staiano RI, Scorziello A, Sirabella R, Boscia F, Adornetto A, Valsecchi V, Molinaro P, Canzoniero LM, Di Renzo G, et al. (2007) BHK cells transfected with NCX3 are more resistant to hypoxia followed by reoxygenation than those transfected with NCX1 and NCX2: Possible relationship with mitochondrial membrane potential. *Cell Calcium* **42:**521–535.

Sirabella R, Secondo A, Pannaccione A, Scorziello A, Valsecchi V, Adornetto A, Bilo L, Di Renzo G, and Annunziato L (2009) Anoxia-induced NF-kappaB-dependent

MOL PHARM
MOLECULAR PHARMACOLOGY
aspet
Downloaded from molpharm.aspetjournals.org by guest on December 1, 2012

upregulation of NCX1 contributes to Ca^{2+} refilling into endoplasmic reticulum in cortical neurons. *Stroke* **40:**922–929.
Taglialatela M, Pannaccione A, Cataldi M, Castaldo P, Secondo A, Iossa S, Di Renzo GF, and Annunziato L (2001) 'Janus face' of nitric oxide action on plasma membrane and intracellular ionic channels. *Arch Gerontol Geriatr Suppl* **7:**379–394.
Taglialatela M, Pannaccione A, Iossa S, Castaldo P, and Annunziato L (1999) Modulation of the K(+) channels encoded by the human ether-a-gogo-related gene-1 (hERG1) by nitric oxide. *Mol Pharmacol* **56:**1298–1308.
Wu A, Derrico CA, Hatem L, and Colvin RA (1997) Alzheimer's amyloid-beta peptide inhibits sodium/calcium exchange measured in rat and human brain plasma membrane vesicles. *Neuroscience* **80:**675–684.

Address correspondence to: Dr. Lucio Annunziato, Division of Pharmacology, Department of Neuroscience, School of Medicine, University of Naples "Federico II", Via Pansini 5, 80131 Naples, Italy. E-mail: lannunzi@unina.it

MOL PHARM
MOLECULAR PHARMACOLOGY
aspet
Downloaded from molpharm.aspetjournals.org by guest on December 1, 2012